

Temperature Field Finite Element Analysis of the Ultra-high Temperature Borehole Incliner based on FOG and Its Optimization Design

Yimin Liu^{*ab}, Jie Wang^a, Weifeng Ji^b, Guangqiang Luo^b

^aSchool of Manufacturing Science & Engineering, Sichuan University, No.24, Section 1, 1st Ring Road(South), Chengdu, China

^bThe Institute of Exploration Technology of CAGS, No.1, Section 2, 1st Ring Road(North), Chengdu, China
153973418@qq.com

This paper puts forward a design method of ultra-high temperature borehole inclinometer based on fiber-optical gyroscope, and this borehole clinometer can be used for measuring the borehole trajectory and its bending value in ultra-high temperature, and the maximum outer temperature is not more than 270°C, and it also can control the internal temperature below 125°C with the help of the metal vacuum flask. The measurement principle is strapdown inertial navigation system, the strapdown inertial navigation system is composed of three axis fiber-optic gyroscopes and three axis accelerometers. In this paper, temperature field of fiber-optic gyroscope is simulated on the basis of considering unified formula of thermal induced error and the heat dissipation of the internal components, the optimization design is verified through the cloud chart of metal vacuum flask temperature distribution. The measuring instrument can work in these deep-holes, and its technology will promote the development of drilling technology.

1. Introduction

In recent years, with the rapid development of the national economy, the shortage of resources and energy has become the major barriers to economic development. In order to get more resources and energy, we can only to explore to the earth deep, so the depth of mineral resources drilling hole is constantly being refreshed. With the development of deep mineral exploration and geothermal resources exploration, the requirement of the drilling trajectory description is becoming more and more accurate. Because of the increase of drilling (well) depth, the temperature in the drilling is also increasing (Beck and Teboulle, 2009). The temperature gradient in the formation is about 3°C/100m, so the temperature of 3000m depth in the oil well can be reach 100°C.

It is well known that with the increase of the depth of drilling well, the bending degree of the drilling hole will be increasing, so the bending of the borehole will have a great influence on the quality and construction safety. Therefore, in the drilling construction the value of the hole bending should be measured in short time, it will provide technical support for the construction (Canuto, 1993). Borehole measurement is a method of measuring the coordinate position of the borehole axis in the underground space with the measuring instrument, at the present stage we commonly measure zenithal angle(the angle between the tangent and the plumb line axis of the measuring point well), azimuth angle(the direction of horizontal projection of the tangent shaft line in the well) and drilling depth, then the space position of the measuring point is calculated by the appropriate calculation method, at last the drilling trajectory data will be obtained(Feng et al., 2015).

In ultra-deep hole drilling engineering, the main technical problems is how to measure the drilling trajectory and ensure the accuracy of the work in the high temperature environment, but it is very short of these borehole trajectory measuring instruments. This paper proposes a borehole trajectory measuring method which is based on fiber-optical gyroscope in in the high temperature and high pressure working environment, and the temperature field error formula of fiber-optic gyroscope is derived which is based on the heat conduction theory and finite element analysis theory, and the simulation model of the ultra-high temperature

fiber-optic gyroscope is established. On the basis of considering the thermal convection of the external environment and the heat dissipation of the internal components, temperature field of fiber-optic gyroscope is simulated and analysed in this paper. Finally, through a large number of heating experiments, the optimization design is verified.

2. Inclinometer measurement principle and its technical parameters

2.1 Borehole trajectory coordinate system and measurement device

Borehole bending Measurement Principle is measuring these key parameters of borehole trajectory, such as zenithal angle(the angle between the tangent and the plumb line axis of the measuring point well), azimuth angle(the direction of horizontal projection of the tangent shaft line in the well) and drilling depth(depth position of the measuring point in the drilling). When these parameters are measured, then the space position of the measuring point will be calculated indirectly by the appropriate calculation method, finally drilling trajectory data will be obtained(Malatip et al., 2012).

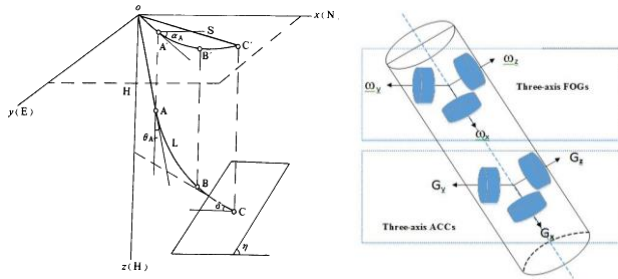


Figure 1: Borehole trajectory coordinate system and the measurement device

As shown in Figure 1, O point represents the position of the drilling orifice, X axis represents the North-South direction, Y axis represents the East-West direction, and the Z axis is the center of the earth, so OABC represents the spatial trajectory of the borehole. For the A point in the figure, the zenithal angle (θ_A) is the angle between the tangent and the plumb line of the point, the azimuth angle (α_A) is the tangent in the horizontal plane of projection and north to the angle, the depth of the hole (H_A) is the distance to the axis of O point in the drilling hole.

2.2 Fiber-optical gyroscope measurement principle

The measurement principle of fiber-optical gyroscope is the Sagnac effect. A beam of light is split and the two beams are made to follow the same path but in opposite directions. The relative phases of the two exiting beams, and thus the position of the interference fringes, are shifted according to the angular velocity of the apparatus. Fringe movement number and the angular velocity of the interferometer and the area of the loop are directly proportional in the Sagnac effect (Shupe, 1980).

The aperture of the loop radius is R, the two beams from the ring light path at the same position in the opposite direction issued at the same time, these two beams communicate at the speed of c in vacuum respectively. When the loop is stationary, the two waves will also return to the launch point, and there is no phase difference; When the loop counterclockwise rotates with the speed of angular velocity ω , these two beams will occur interference after a circle in the opposite direction in the same loop. The optical loop consists of N circles, and the total length of the optical fiber is L, fiber diameter is D, so the Sagnac phase $\Delta\phi$ can be expressed as Eq(1).

$$\Delta\phi = \frac{2\pi LD\omega}{\lambda c} \quad (1)$$

2.3 Measurement method based on strapdown inertial navigation system

The measurement system based on inertial navigation technology is composed of three axis fiber-optic gyroscopes and three axis accelerometers. The three-axis pairwise orthogonal accelerometers measure the acceleration of the three directions, and the displacement of three directions can be obtained by double integrals of acceleration value to time; three-axis pairwise orthogonal fiber-optic gyroscopes measure the rotational speed, and rotation angle can be obtained by integral of time (Singh and Singh, 2015). Through the trajectory calculation model, carrier motion attitude will be calculated by three-axis displacement and three-axis rotation angle.

The Measurement Method which is based on strapdown inertial navigation system involves a variety of coordinate systems, mainly navigation coordinate system XYZ and carrier coordinate system X''Y''Z''. As shown in figure 2, navigation coordinate system XYZ is transformed into carrier coordinate system X''Y''Z'' by Euler variation (Webber et al., 2015).

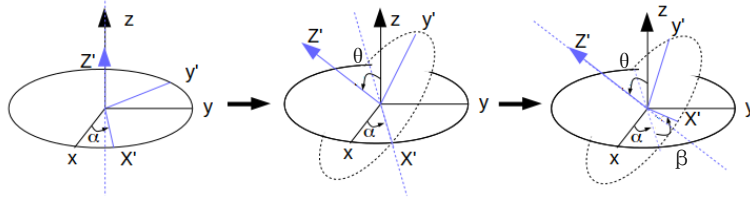


Figure 2: The Euler Variation between Navigation Coordinate System and Carrier Coordinate System

According to the above analysis, the conversion matrix between the navigation coordinate system and the carrier coordinate system is derived.

$$C_n^b = \begin{bmatrix} \cos \alpha & \sin \alpha & 0 \\ -\sin \alpha & \cos \alpha & 0 \\ 0 & 0 & 1 \end{bmatrix} \begin{bmatrix} \cos \theta & 0 & 1 \\ 0 & 1 & 0 \\ \sin \theta & 0 & \cos \theta \end{bmatrix} \begin{bmatrix} 1 & 0 & 0 \\ 0 & \cos \beta & \sin \beta \\ 0 & -\sin \beta & \cos \beta \end{bmatrix} \quad (2)$$

The conversion matrix can be calculated to Azimuth angle α , zenithal angle θ and toolface azimuth β through quaternion algorithm method. In Eq(2), α is rotation angle around the rotating axis. Then solution to ordinary differential equation by fourth-order P-K method, azimuth angle α , zenithal angle θ and toolface azimuth β are shown in Eq(3).

$$\begin{cases} \alpha = \arctan \left[\frac{2(q_1q_2 + q_0q_3)}{q_0^2 + q_1^2 - q_2^2 - q_3^2} \right] \\ \theta = \arcsin \left[2(q_1q_3 - q_0q_2) \right] \\ \beta = \arctan \left[\frac{2(q_2q_3 + q_0q_1)}{q_0^2 + q_1^2 - q_2^2 + q_3^2} \right] \end{cases} \quad (3)$$

2.4 Technical parameters

This inclinometer is composed of memory internal measuring probe and heat and pressure insulation outer tube. Technical parameters of the FOG borehole inclinometer are shown in Table 1.

Table 1: Technical parameters of the FOG borehole inclinometer

Components	Parameters	Value(Range and precision)
Memory internal measuring probe	Zenithal angle	0-90°; ±0.15°
	Azimuth angle	0-360°; ±1.5°
	Working temperature	-10~125°C
	Probe diameter	≤45mm
	Continuous working time	≥96h (Normal temperature)
Insulation outer tube	Pressure-bearing	120MPa;
	Heat insulation	External temperature is 270°C
	Tube diameter	≤75mm

3. Temperature field finite element analysis and optimization design

The fiber-optical gyroscope is the core component of the borehole inclinometer, and the fiber-optic gyroscope has a strong sensitivity to the change of ambient temperature, the change of external temperature will seriously affect the working accuracy of fiber-optic gyroscope, so it is very necessary to study the temperature field of the core mechanism in FOG borehole inclinometer. Due to the terrible working environment in ultra-deep borehole, it is very difficult to simulate the thermal simulation of the internal mechanism by the traditional method of thermal analysis solution, so in this paper finite element analysis method is used in temperature field of the FOG borehole inclinometer. The temperature rise in FOG borehole inclinometer is mainly

determined by two factors: External environment heat convection and internal components thermal dissipation caused by power consumption. Therefore, control of the temperature rise of the instrument is divided into two parts: internal control of thermal dissipation and thermal convection control in the external environment.

3.1 Simulation analysis of FOG temperature field

Due to the ultra-high temperature working environment, metal vacuum flask is additional to the FOG borehole inclinometer. With the help of metal vacuum flask, the inclinometer can work in the temperature of 270°C for a while. The metal vacuum flask is a cylindrical structure, which will protect the instrument into the flask. Its structure mainly consists of three parts: vacuum insulated container part, heat accumulator part and auxiliary part, the structure is shown in figure 3.

The 3D drawings of fiber-optical gyroscope and its solution device in the flask are shown in figure 4.

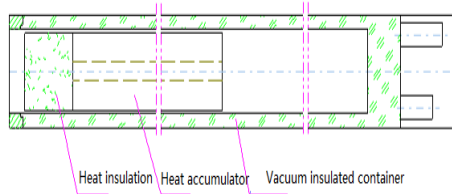


Figure 3: The Structure of Metal Vacuum Flask



Figure 4: The 3D drawings of FOG and its solution device

3.2 Internal heat analysis of FOG borehole inclinometer

The metal vacuum flask is composed of capping, plug, cope absorber (transition body), vacuum bottle body, middle absorber and bottom absorber (transition body), and these components are mainly made of aluminum alloy, 1Cr18Ni9Ti, titanium alloy, 45 steel and other materials. In the process of fiber-optic gyroscope temperature simulation, firstly the parameters of the related materials should be determined. The parameters of the related materials are shown in table 2.

Table 2: The parameters of related materials

No.	Materials	Heat conductivity (W/m·K)	Heat capacity (J/kg·K)	Density (kg/m ³)
1	PCB (FR4)	35.4	962	326
2	Plastic	64	1600	650
3	Fiber ring	0.13	1320	1200
4	Aluminum alloy	238	875	2770
5	45 steel	35.4	46.47	7800
6	Titanium alloy	11.7	858	4470
7	Heat insulator	0.017	550	150
8	Absorber	0.21	1950	900
9	1Cr18Ni9Ti	20	450	7850

ANSYS platform workbench is adopted to determine the convective heat transfer coefficient, and internal heat analysis of FOG borehole inclinometer are like these:

a. Interior heat-power calculation of the FOG borehole inclinometer

In the high temperature working environment, through the calculation of power consumption of different components, the total power consumption include FOG (three axis), accelerometer (three axis) and processing circuit is less than 10W, the details are shown in table 3.

Table 3: The power consumption of main components

No.	Components	Power consumption	Material
1	FOG(three axis)	6W	Aluminum
2	Accelerometer (three axis)	0.9W	Aluminum
3	Acceleration acquisition card	0.2W	Aluminum
4	FOG acquisition card	2W	FR-4
5	High temperature battery	10W	Aluminum
6	Data storage and output module	1.5W	FR-4

Temperature rise Δt can be calculated by Eq(4)..

$$Q_{Total} = Q_v \cdot m \cdot \Delta t \quad (4)$$

In Eq(4), c_v represents the air specific heat capacity at constant pressure in the inclinometer, and its value is $1.35 \sim 1.45 \text{ J}/(\text{kg} \cdot ^\circ\text{C})$. m is quality of the pipe, and its value is 30kg, so the temperature rise Δt is 73.941°C .

b. Heat leakage of metal vacuum flask

The leakage of vacuum flask is transferred from the outside to the inside of the heat, mainly the following two aspects: the first is axial heat conduction through the bottleneck, including solid heat conduction of tube inwall and heat insulation in plug; the second is heat transfer through the heat preservation bottle tube, including the radiation between the inner and outer pipe heat leakage, heat conduction of residual gas and solid heat transfer between vacuum layers. In this paper, total heat leakage is ϕ_{total} , solid heat conduction of tube inwall is ϕ_1 , heat insulation in plug is ϕ_2 , radiant heat is ϕ_3 , heat conduction of residual gas is ϕ_4 . According to Eq(5), $\phi_{total} = 3.325\text{W}$.

$$\begin{cases} \phi_{total} = \phi_1 + \phi_2 + \phi_3 + \phi_4 \\ \phi_1 = \frac{A}{l} \cdot \bar{\lambda} \cdot \Delta T \\ \phi_2 = \frac{S}{l} \cdot \bar{\lambda} \cdot \Delta T \\ \phi_3 = \sigma_0 \cdot A \cdot (T_1^4 - T_2^4) \cdot \frac{1}{n+1} \\ \phi_4 = K \cdot \alpha \cdot (T_1 - T_2) \cdot A \end{cases} \quad (5)$$

3.3 Optimization design and heat simulation results analysis

According to the error formulas in temperature field, the simulation analysis and internal leakage heat calculation, the optimization design of FOG borehole inclinometer reflects in the following aspects:

- (1) Increasing the middle absorber (transition body);
- (2) Replacing partial structure material to absorber material;
- (3) Optimization design of partial structure size.

Based on theoretical design and finite element simulation analysis, in design the size of the metal vacuum flask is 45mm of inner diameter, 56mm of outer diameter, the length of absorber is 400mm, the initial temperature of the internal core is set to 25°C , the initial temperature of the metal vacuum flask outer boundary is set to 270°C , and the working time is set to 4 hours, so according to the third boundary conditions, the temperature simulation results are obtained.

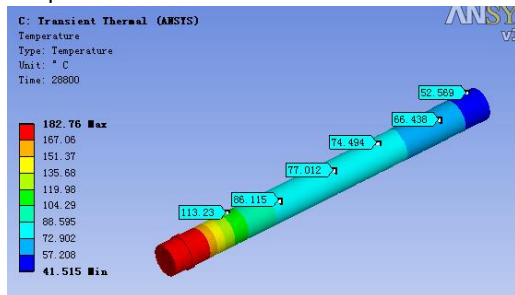


Figure 5: The metal vacuum flask temperature distribution after 4 working hours

The figure 5 is the cloud chart of metal vacuum flask temperature distribution after 4 working hours, through analysis we can come to the following conclusion: after 4 working hours, the general trend of temperature change in the metal vacuum flask is gradually reducing from flask head to bottom, the maximum temperature reach to 113.23°C in the flask head, meeting the requirements of the maximum temperature $< 125^\circ\text{C}$ in the flask; on the other hand, this figure shows the outside temperature is mainly from the flask head into instruments, so the importance of the metal vacuum flask to the fiber-optic gyroscope is proved.

4. Conclusions

This paper puts forward a design method of ultra-high temperature borehole inclinometer based on fiber-optical gyroscope, and its measurement method is based on strapdown inertial navigation system. The

strapdown inertial navigation system is composed of three axis fiber-optic gyroscopes and three axis accelerometers. Then the finite element method is used to analyze the heat transfer characteristics of the ultra-high temperature FOG borehole inclinometer, the Shupe error of FOG is calculated by differential governing equations of heat conduction and thermal boundary conditions, and on the basis of this value, the unified formula of thermal field error is derived. On the basis of considering unified formula of thermal induced error and the heat dissipation of the internal components, temperature field of fiber-optic gyroscope is simulated and analysed in this paper. Finally, through the cloud chart of metal vacuum flask temperature distribution after 4 working hours and a large number of heating experiments, the optimization design is verified, and the importance of the metal vacuum flask to the fiber-optic gyroscope is also proved. This borehole clinometer can be used for measuring the borehole trajectory and its bending value in ultra-high temperature, and the maximum outer temperature is not more than 270°C, and it also can control the internal temperature below 125°C with the help of the metal vacuum flask. This borehole ultra-high temperature clinometer can work in these deep-holes which depth are not exceeding 5000m, and the working range and measurement precision of the measuring instrument in drilling filed are greatly extended, so this measuring instrument will meet the requirement of geothermal energy exploitation, hot dry rock(HDR) research and development, Chinese continental scientific drilling project and mineral resource exploitation in deep layer, which will promote the development and progress of drilling technology.

Acknowledgments

This work is supported by the National Key Scientific Instrument and Equipment Development Project No. 2013YQ050791, and CGS of P.R.China geological survey project No.1212011220169, No.1212011220171.

Reference

- Beck A., Teboulle M., 2009, A fast iterative shrinkage-thresholding algorithm for linear inverse problems(J). *SIAM Journal on Imaging Sciences*, 2(1): 183-202. Doi: 10.1137/080716542.
- Canuto C., Spectral methods in fluid dynamics, Springer-Verlag Press, Berlin. Lefevre, Herve, 1993, The fiber-optic gyroscope, Artech House Publishers, Boston.
- Choi W.S., 2011, Analysis of temperature dependence of thermally induced transient effect in interferometric fiber-optic gyroscopes, *Journal of the Optical Society of Korea*, 15(3): 237-243. Doi: 10.3807/JOSK.2011.15.3.237
- Feng F., Ai C., Xu H., Cui Z., Gao C., 2015, Research on the condition model of drilling fluid non-retention in eccentric annulus, 33(1): 9-16.
- Li G.Z., 2015, The Sustainable Energy and Economy Development in Northeast China, *Chemical Engineering Transactions*, 46: 883-888, DOI: 10.3303/CET1546148.
- Liu Y.M., Wang J., 2015, The research and application of landslide surface crack monitoring method based on laser ranging mode, *Environmental and earth sciences research journal*, 2(2): 19-24.
- Malatip A., Wansophark N., Dechaumphai P., 2012, Fractional four-step finite element method for analysis of thermally coupled fluid-solid interaction problems. *Neuropharmacology*, 33(1): 253-257. Doi: 10.1007/s10483-012-1536-9.
- Shupe D.M., 1980, Thermally induced nonreciprocity in the fiber-optic interferometer, *Applied Optics*, 19(5): 645-655.
- Singh S.N., Singh D.K., 2015, Study of combined free convection and surface radiation in closed cavities partially heated from below, *International journal of heat and technology*, 33(2):1-8. Doi: 10.18280/ijht.330201.
- Vasudevan G., Kothandaraman S., Azhagarsamy S., 2013, Study on Non-Linear Flexural Behavior of Reinforced Concrete Beams Using ANSYS by Discrete Reinforcement Modeling. *Strength of Materials*, 45(2):231-241. Doi: 10.1007/s11223-013-9452-3.
- Webber M., Willig R., Raczkowski H., 2012, Modeling of rate error in interferometric fiber-optic gyroscopes due to stress induced by moisture diffusion. *Journal of Lightwave Technology*, 30(14): 2356-2362. Doi: 10.1109/JLT.2012.2198045.
- Wu L., Li T., Chen Z., Li H., 2015, A new capacitive borehole tiltmeter for crustal deformation measurement and its performance analysis. *International Journal of Mining Science & Technology*, 25(2): 285-290.
- Yang S., Laudanski A., Li Q., 2012, Inertial sensors in estimating walking speed and inclination: an evaluation of sensor error models, *Medical & Biological Engineering*, 50(50): 383-393. Doi: 10.1007/s11517-012-0887-7.